Joint palaeoclimate reconstruction from pollen data via forward models and climate histories

Andrew C. Parnell[a], John Haslett[b], James Sweeney[c], Thinh K. Doan[d], Judy R.M. Allen[e], Brian Huntley[e]

[a]*School of Mathematics and Statistics, Insight Centre for Data Analytics, University College Dublin, Ireland*
[b]*Discipline of Statistics, Trinity College Dublin, Ireland*
[c]*School of Business, University College Dublin, Ireland*
[d]*Novartis Ltd, Ireland*
[e]*School of Biological and Biomedical Sciences, University of Durham, UK*

Abstract

We present a method and software for reconstructing palaeoclimate from pollen data with a focus on accounting for and reducing uncertainty. The tools we use include: forward models, which enable us to account for the data generating process and hence the complex relationship between pollen and climate; joint inference, which reduces uncertainty by borrowing strength between aspects of climate and slices of the core; and dynamic climate histories, which allow for a far richer gamut of inferential possibilities. Through a Monte Carlo approach we generate numerous equally probable joint climate histories, each of which is represented by a sequence of values of three climate dimensions in discrete time, i.e. a multivariate time series. All histories are consistent with the uncertainties in the forward model and the natural temporal variability in climate. Once generated, these histories can provide most probable climate estimates with uncertainty intervals. This is particularly important as attention moves to the dynamics of past climate changes. For example, such methods allow us to identify, with realistic uncertainty, the past century that exhibited the greatest warming. We illustrate our method with two data sets: Laguna de la Roya, with a radiocarbon dated chronology and hence timing uncertainty; and Lago Grande di Monticchio, which contains laminated sediment and extends back to the penultimate glacial stage. The procedure is made available via an open source R package, Bclim, for which we provide code and instructions.

1. Introduction

Quantitative methods in palaeoclimate reconstruction, from pollen in slices taken from a sediment core, were first introduced over three decades ago [8] and have since replaced their qualitative precursors. However, most methods are still

primitive in their modelling of uncertainty. This has greatly inhibited developments on several fronts. In particular, extant reconstruction methods almost never exploit the entire data set available, often ignoring important uncertainties for computational or statistical convenience. As palaeoclimate proxy data are almost always non-standard (non-normal, non-linear, multivariate, etc), this leads to mis-matches between palaeoclimate records across sites, and to a false certainty in the inferences drawn from partial sets of data. Further, real interest often lies in the dynamics of past climate change yet many methods provide a poor basis for inference on such changes. Here we offer a new paradigm, which we refer to as climate histories.

We present software, Bclim, available as an open source R package, as an illustration of our proposed framework. It is the first attempt in palynology at the joint inference of the entire climate history corresponding to a single sediment core. The inputs are:

- A set of fossil proxy data, being pollen counts for each slice.
- The depths of each slice.
- The radiocarbon dates (these may or may not be from a subset of the slices).

In this initial version of Bclim inference is based on a forward model [29] created from a large set of modern data. The complete model is described in Parnell et al. [27], hereafter referred to as P15. The output of Bclim is a large number of stochastic climate histories, each of which is equally statistically consistent with the available data.

We see a forward model [sometimes known as a proxy systems model, 16] as the causal chain through which climate is transformed into proxy data stored in an archive. Our definition is broad, ideally encompassing both deterministic and statistical approaches, but with a clear focus on accounting for uncertainty at each stage. This uncertainty may be due to unknown processes which lend themselves to deterministic modelling, such as the means by which pollen is spread through the local area [e.g. 17], to stochastic processes such as the probability of detecting a particular variety of pollen through a microscope, given that it is present. In our approach we combine the forward model with a simple stochastic climate model via Bayesian inference, which allows us to produce climate histories with narrower uncertainties than using climate dimensions and pollen slices individually.

In this paper we purposefully avoid mathematical notation unless absolutely necessary. The full technical details can be found in P15. Rather, we aim to explain the concepts behind the statistical model we develop so that users of Bclim (and those who work on alternative proxies) can appreciate why these issues are important, and how they are different from previous approaches. We

particularly focus on the output (i.e. climate histories) and the benefit we believe they can offer to those who wish to perform deeper analysis of their proxy data. We emphasise that the use of the software requires no in-depth statistical knowledge of the methods, merely the ability to use some basic R commands and the enthusiasm to find interesting new ways to explore climate histories.

In our first case study [Laguna de la Roya, hereafter Roya; 3], discussed in Section 5.1, the data comprise pollen counts for 28 taxa from 72 slices, and 6 radiocarbon dates. Our target is three specific dimensions of climate over the period 0 to 16 ka BP at centennial intervals. Our three dimensions represent the length of the growing season, the harshness of the winter, and the moisture available to plants. These are the three climate dimensions to which we refer throughout the paper. The resulting output is thus a collection of climate histories, each of dimension $3 \times 160 = 480$. The key points to note are:

- Our forward model contains a simplified mathematical description of how the 28 pollen taxa respond to these three aspects of climate. We create estimates of the climate by inverting the forward model. Inversion is required because we wish to estimate climate from pollen, which is the opposite direction to that of the forward model. We describe the forward model in Section 3.1.
- The 480 values defining each climate history are reconstructed jointly using all slices in the core and all climate dimensions simultaneously. We produce many sets of the 480 values. Each such set is a climate history. Three climate histories are plotted in Figure 1, and discussed in detail in Section 3.2.
- The climate histories are temporally constrained by a model of climate dynamics which also takes account of temporal uncertainty. This part of our model is discussed in Section 4.3.

The paper is structured as follows. In Section 2 we point out in overview how our approach differs to those that are traditionally used. In Section 3 we discuss the three main components at a conceptual level; forward models, joint inference, and the creation of climate histories. This section can be skipped by those who want to avoid any technical detail. In Section 4 we describe the details of our software, Bclim, and the necessary inputs and intermediary steps to the creation of climate histories. In Section 5 we apply our method to two sites as outlined above, and show some of the richer inferential possibilities that are now admissible using climate histories. We discuss further possibilities and extensions in Section 6. Computer code, example tutorials, and the ability to request features or point out bugs, are available at github.com/andrewcparnell/Bclim.

2. Overview of differences between Bclim and previous approaches

Bclim exploits recent developments in statistical methodology in several ways. These developments involve the use of Bayesian methods for joint statis-

tical inference across all available data, and Monte Carlo algorithms to measure uncertainty as explained in Section 3.2. In our case studies the target of inference is a three-dimensional climate time series defined on an arbitrary user-specified time grid. We refer to this multivariate time series as a climate history.

Table 1 provides a toy illustration of the output of our software. Five univariate climate histories are presented in the rows of the table. They are provided on a regular time grid at times 1, 2, 3, 4, and 5. Each history is thus of length 5. Were climate to be bivariate, there would be two values for each time point. The five climate histories are summarised by their column mean and standard deviation in the last two rows. They can be further summarised, as in the last column, by comparing individual differences. Here we have calculated the difference in climate between time 2 and time 1 for each climate history, and summarised them by their mean and standard deviation. The climate histories allow us to estimate, for example, the standard deviation of the difference between times 2 and 1 which would not otherwise be available without the histories. We elaborate on the possible choices and uses of such summaries for more realistic scenarios in Section 3.3 and apply these techniques to our case studies in Section 5.

Time	1	2	3	4	5	time 2 - time 1
History 1	0.44	0.99	1.50	1.84	1.78	0.55
History 2	-0.49	-0.18	0.33	0.46	1.01	0.31
History 3	0.05	0.42	0.76	0.20	0.76	0.37
History 4	0.13	0.33	0.32	0.94	1.34	0.20
History 5	0.31	0.21	0.26	0.27	1.16	-0.10
⋮	⋮	⋮	⋮	⋮	⋮	⋮
Mean	0.088	0.354	0.634	0.742	1.210	0.266
St Dev	0.357	0.423	0.524	0.678	0.383	0.241

Table 1: Five of possibly many climate histories. Climate, for example summer temperature, is first estimated via the joint inversion of a forward model (Section 3.1) then subsequently stochastically interpolated onto a regular time grid, here at time values 1 to 5, to create climate histories. The histories can be summarised via their rows or from the individual climate history values as in the last column where we compute, for each history, the difference in climate between time value 2 and time value 1.

Bclim is based on the Bayesian model discussed in P15. It is one of an increasing number of Bayesian approaches to palaeoclimate reconstruction from proxies [e.g. 37, 19, 36] which involve joint inference and forward modelling. In this paper we sketch the methodology only in outline, referring technical readers to P15. The Bclim approach stands in stark contrast to that provided by very many widely used and cited methods [e.g. 32, 24]. The most widely used, Weighted Averaging Partial Least Squares (WA-PLS), performs reconstructions

separately (i.e. marginally) for each of the chosen dimensions of climate, and for each of the slices in a sediment core. In each case it is using, for each slice, only the corresponding pollen counts for that slice. The reconstruction thus uses only a fragment of the available information. Often only a single 'best' reconstruction is used for each slice. As we elaborate in Section 4, such an approach makes inefficient use of the data and is not to be recommended unless as a crude first step.

More deeply, in WA-PLS and related methods there is no clear modelling of uncertainty. Whilst an attempt at quantifying the uncertainty in each dimension of climate is made (e.g. via a root mean square error of prediction; RMSEP), this is usually a single number which is then used to quantify the uncertainty in the reconstruction. Many users will have the mistaken impression that an underlying normal distribution can be used to interpret the RMSEP, for example by creating the mean plus or minus twice RMSEP. Further, climate dynamics, the implicit focus of many reconstructions, is beyond the reach of the inference. As a simple example, we draw the reader's attention to the mean and standard deviation (the bottom two rows) of the final column in Table 1. While the mean of the difference can be deduced from the difference in the means at times 1 and 2, this is not the case for the standard deviation of the difference, which is impossible to calculate from the column-wise standard deviations.

As well as exploiting more information than typically, the use of joint inference and forward models to produce climate histories provides an entirely new approach to the communication of the uncertainties in reconstruction. Most crudely joint inference will always provide equal or more likely reduced uncertainties in the climate reconstructions compared to slice-by-slice or using individual climate variables. At a more subtle level, the current paradigm, where uncertainty is encapsulated in published error bars (or, worse, in a single RMSEP), provides no basis for comparing, let alone combining, reconstructions which may be similarly uncertain. This itself is an impediment to the wider use of recent statistical methods. As we shall see, the proffering online of a large sample of histories (of which Table 1 is a toy example) may provide such a basis.

3. Forward models, joint inference, and climate histories

In this section we describe the key modelling ideas behind Bclim, leading up to the creation of climate histories. The central issues are: joint reconstruction; specifying forward models and inverting them; incorporating time uncertainty; and the use of Monte Carlo trial and error algorithms to create plausible climate histories. In later sections we explore the Bclim software in greater detail and provide examples. Those who are not concerned with the technical details can skip straight to Section 4 for software details or Section 5 for the case studies.

The main aim of the Bclim software is to find a joint probability distribution of the outputs (aspects of climate) given the inputs (proxy data). This

joint probability distribution is represented, not as an equation which directly gives the probability distribution, but instead via a large set of climate histories which can be summarised to produce means, standard deviations, or, as in the columns of Table 1, richer user-defined outputs. One such richer summary is illustrated in the rightmost column of Table 1. Here we investigate the change in climate between times 1 and 2. This involves computing, for each history separately, the corresponding simple differences and subsequently summarising them.

The probability distribution defined by the climate histories is joint in the sense that the individual histories are statistically consistent. That is, not only are they consistent with the relationship between pollen and climate (founded in the forward model, discussed below), but they borrow strength from neighbouring slices and agree with explicit assumptions concerning climate dynamics. Furthermore, we can reconstruct multiple aspects of climate simultaneously (not shown in Table 1) and borrow strength between the climate dimensions.

3.1. Forward models for pollen

The first step in our Bclim modelling process is the creation of a statistical representation of the data generating process, i.e. the process by which pollen records arise in (indirect) response to changing aspects of climate. Often this is called a *forward model*; these are increasingly proposed and used in palaeoclimate reconstruction, particularly in tree-ring studies [e.g. 35, provide an approach which, like ours, allows for probabilistic inversion], and more recently in sea level reconstruction [15]. A review of earlier forward models for pollen data can be found in [25]. Forward models typically have the advantage that they can be decomposed to model several processes involved in generating and archiving the proxy data in response to climate. The Bclim forward model, given past climate, will generate pollen data as output. This forward model will typically require the estimation of some additional internal parameters, for example the sensitivity of a particular pollen taxon to an aspect of climate. The technical task provided by Bclim is then to *invert* the forward model.

The forward model we use can be decomposed into a number of sequential steps:

1. Plants are responsive to changes in certain aspects of climate. In Bclim, these are: the harshness of the winter; the accumulated warmth of the growing season; and the moisture available to plants. These three aspects form our multivariate climate.
2. The relationship between pollen production and its response to this multivariate climate is assumed to have remained constant throughout the period over which pollen has been collected, and to apply still to modern pollen generation. Since the corresponding modern climates are known,

this permits the detailed calibration of this relationship. In Bclim this is an external step, fully described in [29][1].

3. As deposition occurs the archive [the medium in which the proxy data are stored; 16] is collecting dateable material which can provide a basis for (possibly uncertain) dating of all sediments.
4. Pollen abundance is measured by experts counting grains for a slice of a core under a microscope. This process induces uncertainties, in that occasionally grains will be missed, pollen mis-identified, and abundances mis-reported, and can be modelled stochastically.
5. Dateable material is measured, most commonly through radiocarbon, which also involves a stochastic calibration process. Additional uncertainty occurs when interpolation is required to find the age of undated slices.

The forward model in Bclim concerns all steps except 3 and 5. Steps 3 and 5 refer to the sedimentation process, for which we use the previously developed Bchron forward model [18, 26], discussed more fully in Section 4.2.

The steps above allow the forward model, given the aspects of climate specified in (1), to proceed sequentially with the end result being a set of stochastic pollen counts for each slice. It is a causal, and potentially rich, approximation to the steps required to generate realistic proxy data from dynamic climate.

In this version of Bclim, as in all modelling, the approximations are simplifications of reality. In particular, vegetation composition may change in response to changes in other climatic or non-climatic factors, potentially leading to biases in the modelled relationships and hence in the reconstructions. In some regions, and during more recent time, anthropogenic interference with the vegetation may have led to changes which the model will falsely attribute to climatic change. More generally, our models do not account for potential lags in the responses of vegetation to climatic changes that may result from limitations upon species' migration rates and/or the requirement for a disturbance episode to facilitate both these migrations and the associated changes of vegetation composition [see e.g. 12]. The model assumes that changes in vegetation, and hence in the pollen recruited to sediments, occur immediately following a change in climate. Given the evidence that the lags in vegetation response are generally much less than temporal uncertainties associated with the use of 14C dating [see e.g. 34, 40], we believe that this is an acceptable simplification. Furthermore, we envisage that richer approximations, accounting both for the influences of other factors and for the mechanisms of ecological processes, will be a major focus of future research.

Given the forward model as specified above, reconstruction can be seen as its inverse. Conceptually this involves running the steps in reverse to get from

[1] In the current version of Bclim this calibration is beyond user access. The step is fully described in Section 2.1 of P15

observed pollen data and dates (output from the forward model) to the unobserved climate (input to the forward model). Bclim is one procedure to achieve this. The unknown inputs to the forward model become the outputs from Bclim. The unknown outputs from the forward model (pollen data and dates) are the known inputs to Bclim.

3.2. Creating plausible climate histories

The logistics of creating climate histories via an inverted forward model are highly technical, particularly if they are to be computationally efficient. However the target of the inference can be stated in terms of the joint conditional probability distribution of the unknowns (aspects of climate) given the knowns (proxy pollen data, dates). We believe the best and simplest way to perform the inversion and to compute this distribution is via Bayesian inference. Bayesian inference allows for the forward model (in Bayesian parlance, the likelihood) to be combined with assumptions about climate dynamics (the prior distribution) to produce climate histories (the posterior distribution).

The target posterior probability distribution may be formally specified as:

$$\underbrace{p(\text{climate histories given all data})}_{\text{posterior}} = k \times \underbrace{p(\text{all data given climate histories})}_{\text{likelihood}} \times \underbrace{p(\text{climate histories})}_{\text{prior}}$$

where $p()$ is a multivariate probability distribution and k is an irrelevant constant. The likelihood is the forward model, and the prior can be seen as constraints on the forward model to produce 'realistic' climate histories. Both the likelihood and the prior are informed by knowledge beyond just that of the proxy data including, but not limited to: modern training data; theory about climate dynamics; theory about sedimentation.

Once the likelihood and prior are specified, the model needs to be fitted using a computational algorithm. Most algorithms for fitting complicated Bayesian models create sample values (equivalent to our climate histories) from the posterior distribution rather than calculating it directly. Furthermore they often work via trial and error, guessing climate histories and 'scoring' them against the likelihood and the prior. Histories which score highly will be repeated often in the posterior distribution, whereas histories with low score will only occasionally be included. Thus each set of sample values from the joint posterior distribution is equally likely given the observed data.

3.3. Using climate histories for richer palaeoclimate inference

In Table 2 we provide a slightly more detailed version of our Table 1 by including the slices from which the pollen data were obtained. These slices are an explicit part of the model, but were previously hidden when we considered just

the resulting gridded output. We here assume their known ages to be 2.9, 4.6 and 4.8. The rows of the toy illustration in Table 2 are now samples of a random variable of dimension eight, being made up of estimates of climate at the times of the three proxy slices and five further time grid points. These latter grid points can be arbitrarily chosen by the user, and so we can discard the climate estimates at the observed slices if we wish (as in Table 1). In Section 5.1 (Roya) the time grid is set such that the climate histories are of dimension 480, as they also encompass three dimensional climate. Such high dimensional probability distributions of random variables are impossible to visualise, even if available as explicit formulae. Indeed the only practical usefulness of such a formula is the knowledge that we may use it to construct low dimensional summaries (often also probability distributions) of the elements, such as that given in the row means of Table 2.

Slice			Slice 1			Slice 2	Slice 3		
Time	1	2	2.9	3	4	4.6	4.8	5	time 2 - time 1
History 1	0.44	0.99	1.34	1.50	1.84	1.68	1.87	1.78	0.55
History 2	-0.49	-0.18	0.05	0.33	0.46	0.99	1.05	1.01	0.31
History 3	0.05	0.42	0.52	0.76	0.20	0.59	0.85	0.76	0.37
History 4	0.13	0.33	0.02	0.32	0.94	0.98	1.20	1.34	0.20
History 5	0.31	0.21	0.16	0.26	0.27	0.64	0.96	1.16	-0.10
⋮	⋮	⋮	⋮	⋮	⋮	⋮	⋮	⋮	⋮
Mean	0.088	0.354	0.418	0.634	0.742	0.976	1.186	1.210	0.266
St Dev	0.357	0.423	0.552	0.524	0.678	0.435	0.403	0.383	0.241

Table 2: Five climate histories together with their climate estimates at the time slice values. Climate, for example summer temperature, is first estimated via the joint inversion of a forward model (Section 3.1) at three slices, given at times 2.9, 4.6 and 4.8, then subsequently stochastically interpolated onto a regular time grid, here at time values 1 to 5, to create climate histories. Table 1 is then created by removing the columns corresponding to the slices. As before, the histories can be summarised in any desirable fashion.

If we focus on a single column of Table 2, for example the first, we find samples of a univariate random variable representing the first dimension of climate at time $t = 1$. One useful summary of this is its mean value. This is in fact an estimate of the posterior mean of climate at time $t = 1$ given all available data. If rather than 5 we had 10, or 10,000, rows in Table 2 this estimate would improve. An estimate of the posterior standard deviation, or any other chosen summary, is also available. Because the histories are created via simulation, we can choose an arbitrarily large number upon which to base this estimate.

A key aspect of this approach is that there is no assumption that any of the probability distributions are normal. On the contrary, the distribution is often multi-modal. Estimates of any aspect of the distribution of climate at

time $t = 1$ are similarly available. More generally, estimates of any univariate marginal distribution of the multivariate random variable are available from the columns of Table 2, and the estimates can be made arbitrarily precise by adding rows to the Table. Thus the means and standard deviations provided in the bottom two rows may in fact be poor summaries of the histories, and better alternatives (e.g. highest posterior density regions, commonly used for calibrated radiocarbon dates) may be sought.

If we focus instead on the first two columns, we have access to the bivariate marginal distribution of the climate variables at times $t = 1$ and $t = 2$, representing our knowledge, in the light of the available data, of the change in the first dimension of climate. One natural way to pursue this is to consider the distribution of the differences. The rightmost column illustrates the natural route to this: first, form the differences row-wise; second, summarise these differences.

It is worth pausing to consider this latter example in detail, for it illustrates a crucial difference between joint and marginal reconstruction. Recall that joint inference is a central contribution of this paper; the vehicle for this is climate histories. The estimate of the mean difference is of course equal to the difference between the two marginal means (as can be verified by comparing the first difference of the penultimate row). But the estimate of the standard deviation of the difference is not available without the histories, unless there is no correlation over time. With histories, such standard deviations can be trivially computed for all such differences. The standard deviations of such first differences are referred to in Section 4.3 as volatilities.

We believe that the natural route for the user in studying past climate dynamics begins with the construction of climate histories. Subsequently the user will summarise these. These summaries may include means, standard deviations, differences, maxima, etc. All are available with quantified estimates of uncertainty. In Section 5 we provide illustrations where we explore the first differences and the main modes of climate change. We do this by first computing, for each history, absolute first differences. Secondly we compare these, again for each history, through means and standard deviations.

4. The Bclim software and its practicalities

We now describe, without technical detail, how we take pollen and chronological data as input and output climate histories. There are three essential steps:

1. The creation of single slice climate clouds. These are multivariate estimates of three dimensional climate at each slice in the core, based *only* on the information at that slice and the forward model. They do not borrow strength between slices.

2. The creation of a set of chronological histories from the dated material and their associated uncertainties. These are obtained using an age-depth model. We use Bchron [26, 18] for this purpose.
3. The stochastic interpolation and smoothing of the single slice climate clouds. This constrains the climate cloud to exhibit only 'reasonable' climate change given the chronological histories and the prior distribution on climate. This step produces the climate histories in a joint framework.

In Bclim we offer specific modelling choices for each of these steps, as discussed below. However we emphasise that other, perhaps radically different, modelling choices could be proposed and used within this structure.

Bclim takes as input two files. The first contains fossil pollen counts where each row is a slice in the core and each column is one of 28 pre-determined taxa. The counts can be raw or re-scaled. The second is a file of chronologies from a suitable chronology modelling programme. This file needs to have a large number of rows (the default is 10,000 but it can be higher or lower) each of which represents a sample chronology that is consistent with the dating evidence. Each column should correspond to a depth in the core at which pollen has been counted. The number of rows in the pollen counts file should be the same as the number of columns in the chronology file. The chronologies file can be created using any Bayesian chronology programme (e.g. Bchron; OxCal, [14]; Bacon, [9]). We use Bchron as it has been designed for input into Bclim. Indeed, the chronological histories can be thought of as analogous to the climate histories. We detail the Bchron step below, but really this is an extra step to be pre-computed outside of the Bclim package.

4.1. Step 1: Creating single slice climate clouds

This first step focusses on the inversion of the forward model at single slices. The objective is the reconstruction (here probabilistic), for each slice independently, of the three dimensional climate that is statistically consistent with the single set of pollen data at that slice. Subsequently the constraints of a simplistic climate model will be used to refine these probabilistic reconstructions. Formally the objective here is a multivariate distribution:

$$p(\text{climate at slice } i \text{ given pollen at slice } i).$$

Note the distinction from p(climate at slice i given pollen at all slices), the interpretation given to the slice i columns in Table 2. The technical reader is referred to [29] or [31] for full details of this step.

Conceptually, three dimensional climates are proposed, *independently* for each slice. Each is contrasted with its associated pollen record. Once again, those that are deemed to be relatively statistically inconsistent, in the sense of the forward model, are rejected with high probability; and conversely accepted

if consistent. Slice-by-slice reconstructions may then be thought of either as a distribution p(climate at slice i given pollen at slice i) or as a large sample of three-dimensional climates for each slice. The latter can be visualised, when combined with chronological uncertainty and plotted on a time vs climate graph (as in Figures 1 and 3), as a set of clouds, one for each slice. Each plot is of a single dimension of climate, but we remind the reader that these slice-by-slice reconstructions are *joint* across climate dimensions.

The likelihood used to create the single slice climate estimates is built on a forward model from climate to pollen (as previously discussed in Section 3.1). This involves a statistical model that has been calibrated on modern data. The calibration aims to take account of the way that differing pollen taxa respond to climate. A byproduct of this modelling is the creation of response surfaces [*sensu* 7, 21] in three dimensional climate space. Since the modern data are themselves imperfect, the uncertainty in the climate-pollen relationship will cascade through to the creation of probabilistic single slice climate clouds.

4.2. Step 2: Chronological histories via Bchron

When the dates associated with the slices are taken to be known we may move directly to step 3, armed with the slice-by-slice reconstructions. When, as typically, the dates are known only through, e.g. the radiocarbon dating of the material in a few sampled slices, it is wise to acknowledge this uncertainty through a chronology module. Bclim uses the Bchron software for this. The methodology underlying Bchron has been described elsewhere [18]. The R package, including a vignette describing its use, is available at cran.r-project.org/web/packages/Bchron. A pre-release version which allows for the reporting of bugs and requests for new features is available at github.com/andrewcparnell/Bchron. Here it is sufficient to give an outline sketch.

Associated with the slice-by-slice pollen data are sets of known depths and true but unknown dates. These reflect the sedimentation history of the archive which holds the pollen, and in particular the law of superposition, where deeper necessarily means older. Bchron acknowledges the uncertainty of the radiocarbon dating and uses a special type of stochastic linear interpolation to generate multiple stochastic chronologies for the entire set of pollen slices. Each of these is statistically consistent with the dating and the relationship with neighbouring slices.

More generally, Bchron can be though of as providing a forward model for the relationship between depth and dates. Given some constraints on sedimentation (e.g. superposition, hiatuses) we can generate plausible dates. As with Bclim we have to invert this forward model as our input is the dates (with uncertainties) and our output will be sedimentation histories, exactly analogous to the climate histories Bclim creates.

4.3. Step 3: Statistical modelling of climate dynamics

The task in this step is to construct entire sets of three-dimensional climate on an arbitrary time grid. The inputs for this step are the estimates of slice-by-slice climate (step 1) and chronology (step 2), both of which are provided with uncertainty. The outputs are climate histories similar to those given in Table 1, but on a larger scale with more climate dimensions. It is of course feasible to create crude climate histories by repeatedly sampling from the climate/chronology estimates in each slice (corresponding to sampling from the blue clouds in Figure 1, discussed in Section 5.1). However, this is likely to lead to climate histories that are physically unlikely in respect of temporally-local variability. The climate information in many of the pollen samples individually is weak, and independent sampling can, by chance, result in adjacent pairs of slices that have very different values for the corresponding climate variables. Instead we use a statistical model which aims to approximate real climate dynamics. It is in fact a 'smoothing' approach, though our method may produce histories which show minimal smoothness, to constrain the slice-by-slice reconstructions. The practicalities of this step are outlined in our case studies.

A crude version of the algorithm proceeds by comparing proposed histories from the slice-by-slice reconstructions with a stochastic model of climate dynamics. Each such proposal is scored via the prior. Once again we reject, with high probability, the histories that have relatively low scores, and conversely accept most of those with relatively high scores. The resultant accepted histories become the columns of a table such as Table 1. In fact, in the case of the very simple yet flexible climate model adopted in Bclim, each climate history is scored according to the first differences for each dimension of climate. The vast majority of proposed histories will contain at least some first differences that are far too large in this sense, given the computed time differences; as such, these will be rejected with high probability. Those few that are accepted are statistically consistent with the forward model, the pollen spectra at each slice, and the chronological data.

The statistical model of climate dynamics is based on each climate dimension following a standard random walk (strictly speaking a Brownian Motion) in continuous time. It extends this basic model by allowing the variability between each time increment to itself be dynamically changing in time. This model is a form of stochastic volatility model [6]; the type we use being known as a Normal Inverse-Gaussian process. The standard deviation between time increments is known as the volatility. Large volatility during a certain time period indicates rapid changes in climate, small volatility corresponds to smooth climate behaviour. The statistical model of climate dynamics aims to estimate the changing volatility over time as part of the creation of the climate histories.

The stochastic volatility model by itself does little to constrain the slice-by-slice changes in climate; it merely allows for the appropriate modelling of

the uncertainty. To constrain the climate dynamics properly, we use the standard method of placing informative prior distributions on the parameters of the probability distribution to control the volatilities. More specifically we place restrictions so that the volatilities of the climate histories match the volatilities displayed over an equivalent time period as shown, for example, by the δ^{18}O record from the Holocene period of the GISP2 ice core [30]. To be clear, we are not restricting our reconstructed climates to match that of an ice core record. We are merely stating that the volatilities (standard deviation in climate change over time) should be broadly consistent with an ice core record. The full technical details are in P15.

To finish, we plot the climate histories against the time grid to provide a picture of the joint distribution of climate over time for each climate dimension individually. We also plot the individual slice climate clouds as these provide some information about the evidence for specific climate values provided by each layer in the core. In general, the climate histories will form a path through the most likely parts of the climate clouds. We summarise the climate histories at each time grid point to produce marginal summaries, which we term the *climate ribbon*. In all our case studies it is the case that the climate ribbon is substantially less uncertain than the individual slice-by-slice reconstructions. It is important to remember that the climate histories are the basis for all subsequent analysis of the palaeoclimate reconstructions. We sometimes thus include one or more representative climate histories in the plots.

5. Case Studies

We now present two illustrative examples of the Bclim methodology and the use of climate histories to produce richer inferential products. The first example, Laguna de la Roya, has radiocarbon dated sediments and so we must account for time uncertainty. The second example, Monticchio, contains laminated sediments and far reduced (but still present) chronological uncertainty. In both cases our goal, aside from reconstructing our three dimensions of climate, is to find the century or millennium with the largest change in climate over the reconstructed period.

5.1. Roya

Laguna de la Roya is a small (ca. 2.5 ha) mountain lake situated in the Sierra de Cabrera in north-west Spain (42°13'N, 6°46'W, 1608m a.s.l.). The sediments were cored in September 1991 using a piston corer operated from a raft; a core of 817cm being obtained. Pollen counts were made for 72 sediment slices and plant macrofossils extracted, identified and counted from 30 samples. AMS radiocarbon dates were obtained for six samples of bryophyte macrofossil material. [3] published the pollen and macrofossil diagrams, radiocarbon chronology (uncalibrated) and quantitative response surface based

reconstructions of three bioclimatic variables, made using inferred biome and macrofossil-based constraints on analogue selection, along with full details of the site and of the methods used. They estimated the record to extend to 14,559 ^{14}C yr BP and recognised six local pollen assemblage zones.

In discussing their record, [3] drew attention to problems with the reconstructions of mean temperature of the coldest month (MTCO) and of annual thermal sum above 5°C (GDD5), especially noting the anomalously warm reconstructions for some samples from the late-glacial section of the record. Their chronology also gave a rather young date of 9,853 ^{14}C yr BP for the marked palynological and sedimentological changes interpreted as representing the onset of the Holocene.

We have applied Bchron to the radiocarbon dates and Bclim to the pollen data for Roya (Figure B.8, Appendix), the latter providing an age-depth relationship shown in Figure A.6 (Appendix) and the former the reconstructions of the same three bioclimatic variables (Figure 1) on a centennial time grid. Included in each plot are three 'most representative' climate histories, constructed by finding the histories that are the median Euclidean distance away from the time-wise overall median. These are included to give a flavour of how the individual climate histories actually look and where they lie within the climate ribbon summary. Finally, we include plots of the first differences, summarised by their means and standard deviations, and coloured according to the signal to noise ratio, in Figure 2.

There are some features of Figure 1 which are clearly unrealistic, and are side-effects of the first generation, proof-of concept nature of our Bclim model. The first of these is the trumpeting out of uncertainty as we reach the present. Future versions of Bclim could allow the user to input constrained climate values for the present. Another is the possibility for the climate ribbon to lie outside the plausible range of the climate variable (see bottom panel of Figure A.6 period 0 to 1k BP). This arises from the normally-distributed nature of the stochastic volatility climate model discussed in Section 4.3. Again, future versions may allow for a richer climate model surrogate that respects the bounds of the climate variable in question. We ignore these issues in our remaining interpretations.

Figure 1 shows that the uncertainty in the single-slice climate clouds (plotted in blue) is much greater for the late-glacial part of the record, extending to values higher than present for the two temperature-related bioclimatic variables. However, the marginal summaries for these variables (the climate ribbon, plotted in red) made from the climate histories reconstruct the late-glacial climate as cooler than present with respect to MTCO and relatively cool in terms of GDD5. Most strikingly, however, the reconstructed late-glacial climate is very much drier than present, with the ratio of Actual to Potential Evapotranspiration (AET/PET) rising to values similar to the present in two discrete

steps centred upon 15 and 12 ka BP (Figure 2). The Younger Dryas interval is marked by a slight reduction in AET/PET compared to the late-glacial interstadial, but without clear evidence of cooling in either temperature-related variable.

Figure 2 presents the mean ± 1 standard deviation of the differences for each of the three bioclimatic variables. Such a summary is readily constructed from the climate histories. We further colour the plot via the signal to noise ratio (SNR; calculated by dividing the time-wise mean difference by the standard deviation of the time-wise differences) which enables us to highlight periods of clearly identified rises and falls in the three climatic variables. The SNR values in general are low (much less than 1) indicating that the signal here is weak, likely due to the uncertainty in the chronology and the reconstructed climate variables.

All three variables show some evidence of change just after 12 ka BP, though this is most pronounced in moisture (AET/PET). This appears to encompass the Greenland ice-core derived date of 11,703 b2k [28] for the onset of the Holocene, and clearly corresponds to the major local climatic and vegetation transition from the late glacial to Holocene. AET/PET further shows a major change in the interval between *ca.* 15.5 and 14.5 ka BP (Figure 2 lower panel), although the exact timing and nature of this change differs between the three bioclimatic variables. This appears to occur a few centuries before the Greenland ice-core data for the onset of GI-1 of 14,692 b2k [28]. Whilst the systematically earlier ages at Roya may simply reflect the uncertainties both in its radiocarbon-derived chronology and in the INTIMATE event chronology, they may also indicate that these shifts in the climatic system were time-transgressive, as others have suggested [23]. The sequencing of peak changes in the three bioclimatic variables may provide insight into the underlying changes in the climatic system. A time-transgressive northward shift of the Polar Front in the North Atlantic might well first influence regional temperatures, with moisture availability increasing only a few centuries later when a sufficient part of the source area for precipitation had warmed.

A final transition identified from Figure 2 is a clearly identifiable decrease in GDD5 and MTCO at around 1.3 ka BP, and a smaller corresponding rise in AET/PET. It is tempting to speculate that this may correspond to Bond Event 1 dated to 1.4 ka BP [10]. Such a clear link between a climatic event in north-west Iberia and in the North Atlantic would not be surprising. Furthermore, given that Bond Events are characterised by increases in the flux of ice-rafted debris and cooling of Atlantic surface waters, an impact principally upon temperatures in north-west Iberia, rather than upon moisture availability, is a consistent finding.

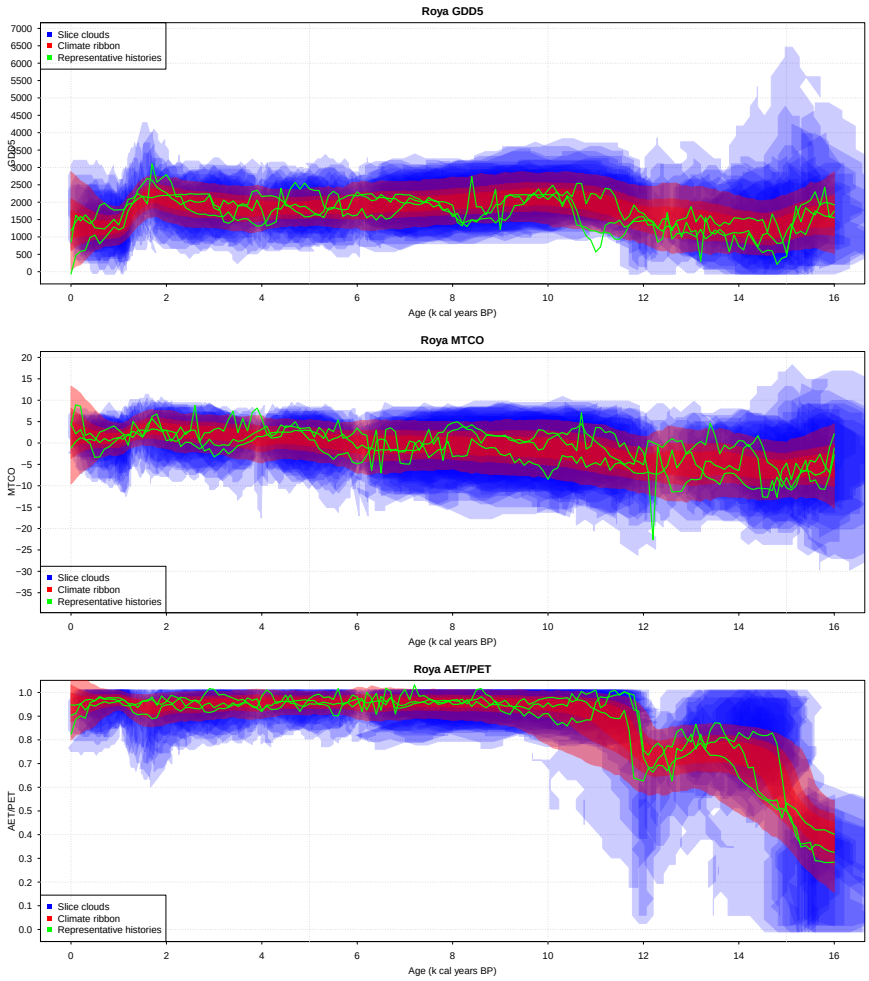

Figure 1: Roya reconstructions of Growing Degrees Days Above 5°C (GDD5), Mean Temperature of the Coldest Month (MTCO), and Ratio of Actual to Potential Evapotranspiration (AET/PET). The blue blobs represent the slice clouds (95% confidence region) whilst the red represents the climate ribbon; time-wise 95% confidence intervals. The darker shading represents the 75% and 50% intervals. Overlaid are three green 'most representative' climate histories.

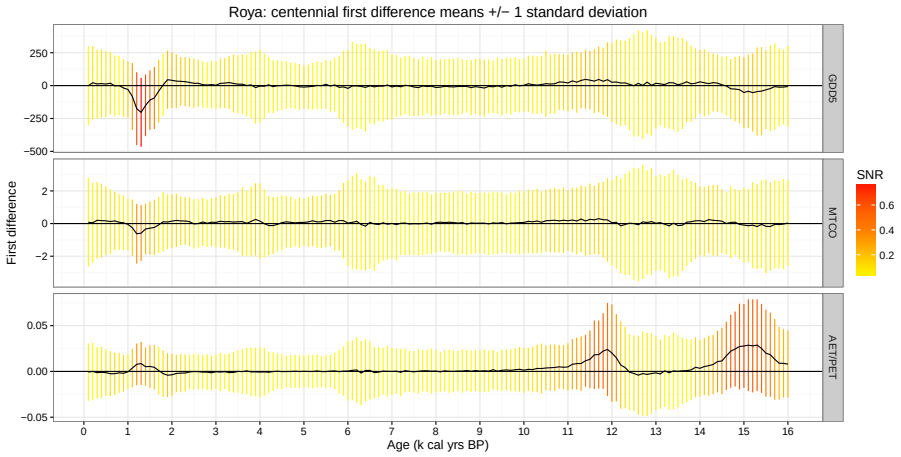

Figure 2: Roya plot of time-wise first difference mean +/- one standard deviation. Each time slice is coloured by its signal to noise ratio (SNR). The darker colours indicate a more identifiable location of change. Positive values indicate increases in the climate variable, whilst negative values indicate decreases. The solid black line indicates the mean of the first differences.

5.2. Monticchio

Lago Grande di Monticchio is a medium-sized maar lake (41 ha) situated in the crater of Monte Vulture in Basilicata, southern Italy (40°57'N, 15°37'E, 656m a.s.l.). The sediments have been cored on several occasions since the first core was taken in 1982 [38]; the basal sediments were reached in 2000 giving an overall sediment column of 102.3m [13]. The sediments are in large part annually laminated, as well as containing numerous tephra layers [41]. The site chronology is based upon layer counting validated by independent tephrochronological ages and extends to a minimum basal age of 132.9 ka BP [13]. The reported age error for the site is 1.5% of the mean age, so we simulate uncertain chronologies from the estimated mean layer counts via this rule. The chronology (shown in Figure A.7) is considerably less uncertain than that of Roya.

A pollen record for the entire sediment sequence has progressively been developed and published as more of the sediment column has become available for analysis [Figure B.9; 38, 39, 22, 5, 4, 1, 2]. Response surface based quantitative palaeoclimate reconstructions made from the pollen record have been included in most publications. The record now available and used here comprises pollen counts and age estimates for 924 samples. It commences during the end of the penultimate glacial stage, spans the last interglacial and last glacial stages, as well as the Holocene, and is continuous to the present day. The striking features of the record are the millennial palaeovegetation changes during the last glacial stage that strongly parallel the record of alternating stadials and interstadials seen in Greenland ice cores [5]. There are also striking differences between the

last interglacial and Holocene in terms of both palaeovegetation development and inferred palaeoclimate.

The Bclim reconstructions for the three bioclimatic variables are presented in Figure 3, based on a centennial time grid. Once again very large uncertainties are shown by the single-slice climate clouds (plotted in blue) for some variables during glacial centuries, consistent with the anomalous palaeoclimate reconstructions for some samples obtained by Allen et al. [4]. The climate ribbons for these variables (plotted in red) made from the climate histories, however, give much clearer patterns. The strongest and clearest patterns of change are in AET/PET. This should not be surprising given the sensitivity of moisture availability (to the latitude in which Monticchio lies) to shifts in the predominant latitude of seasonal storm tracks that are likely to accompany changes in Atlantic surface temperature and circulation. Gaps in the chronology occur at approx 27.7–30.3 ka BP and 38.7–40.1 ka BP, and as such there is a considerable increase in uncertainty in the red climate ribbons during these periods. Whilst we show these periods in Figure 3 for completeness, for our subsequent discussion we ignore them for the purposes of interpretation.

Given the length and complexity of the Monticchio record, it is particularly advantageous to be able to summarise the climate histories in various ways. This can once again be done via the means and standard deviations of the first differences (Figure 4). We present these as millennial first differences using a sliding window approach moving along a centennial time grid. The plots are again coloured by the signal to noise ratio (SNR). These values are much higher than the Roya version (Figure 2), largely due to the extra precision in the chronology.

Focusing upon peaks with high signal to noise ratios, GDD5 shows a strong millennial increase during the millennium centred on 110 ka BP (Figure 4). This increase was accompanied by marked decreases in both MTCO and AET/PET, the peak rate for the latter also being during the millennium centred upon 110 ka BP, whilst the peak rate for MTCO lagged by 500 years, falling during the millennium centred upon 109.5 ka BP. These changes correspond to the transition from the Last Interglacial to the Melisey 1 stadial, a transition that is closely preceded by the short-lived Woillard Event [13]. Although the palaeoclimatic reconstructions for the Melisey 1 stadial show relatively high uncertainty (Figure 3), there is nonetheless evidence for a markedly continental climate during this interval, with strong temperature seasonality and growing season moisture deficiency.

GDD5 had its most rapid millennial increase during the millennium centred upon 91.3 ka BP. This increase was again accompanied by parallel decreases in both MTCO and AET/PET, with peak rates for both during the millennium centred upon 91.5 ka BP. These changes are associated with the transition from the St Germain 1 interstadial to the Melisey 2 stadial [13], during which pollen taxa characteristic of steppic conditions increased in abundance prior to the very

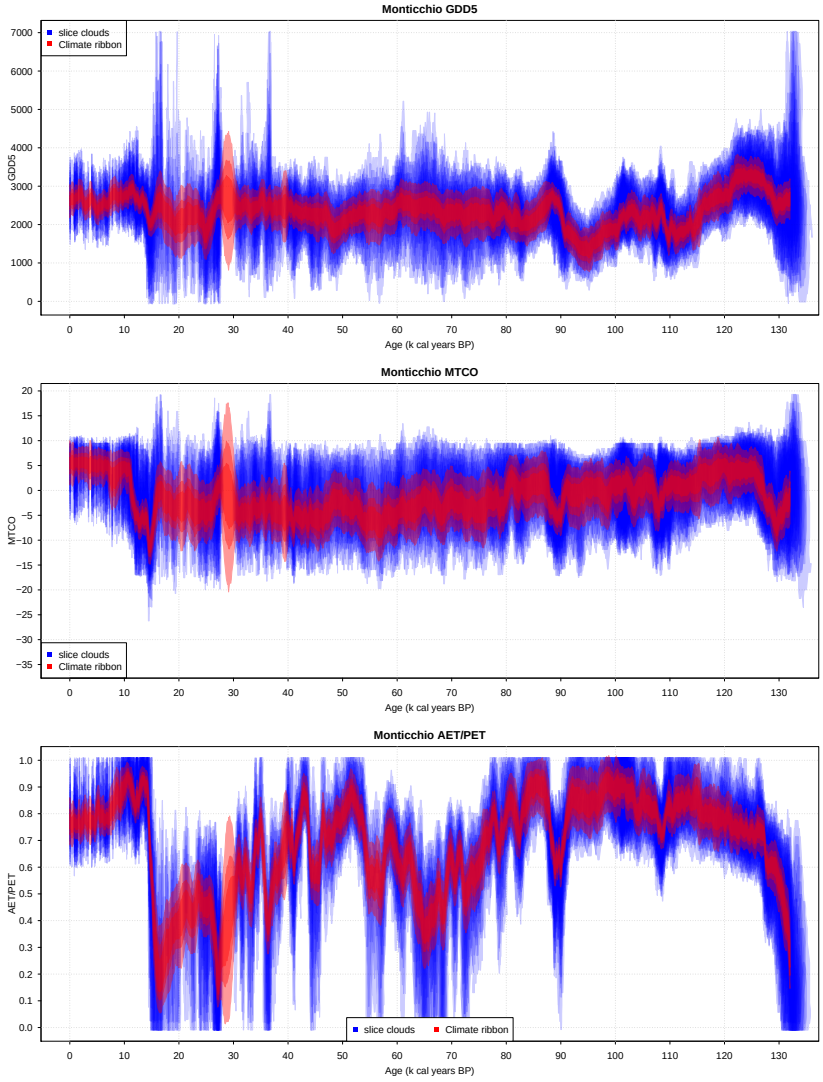

Figure 3: Monticchio reconstructions of the three climate dimensions GDD5, MTCO, and AET/PET. The blue areas represent the 95% credible regions of the slice clouds whilst the red ribbons represent the 95% confidence intervals for each time grid point on a centennial time grid. Darker regions indicate the 75% and 50% regions.

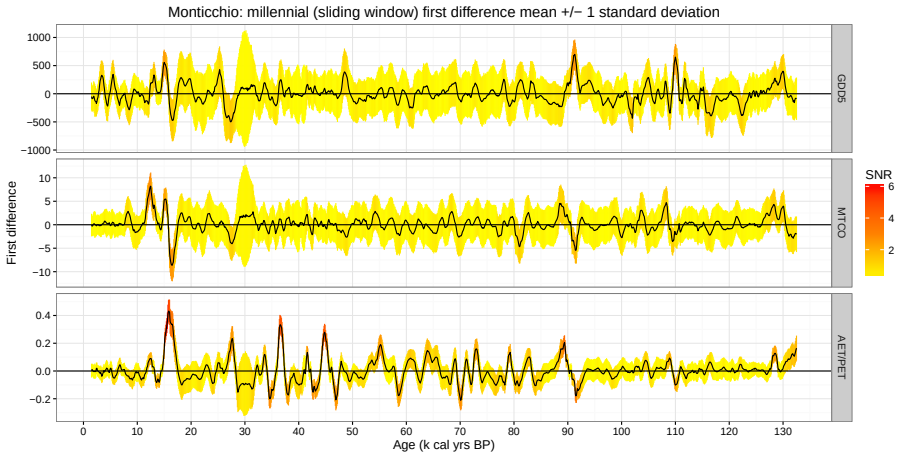

Figure 4: Monticchio plot of time-wise first difference means +/- one standard deviation. The differences are calculated between each millennium using a sliding window approach along a centennial grid. Each time slice is coloured by its signal to noise ratio (SNR). The darker colours indicate a more identifiable location of change. Positive values indicate increases in the climate variable, whilst negative values indicate decreases.

marked decrease in tree pollen abundance at the end of the interstadial. Although the palaeoclimatic reconstructions for the Melisey 2 stadial again show relatively high uncertainty, there is nonetheless clear evidence for a markedly continental climate once again during this interval.

The most rapid millennial decrease in GDD5 was during the millennium centred on 27.4 ka BP. This shortly lagged a marked decrease in MTCO centred on 27.6 ka BP and an increase in AET/PET centred on 27.7 ka BP. These changes apparently marked the onset of a stadial interval, with all three variables subsequently increasing after about two millennia, peak rates of increase marking the end of the stadial centring on 25.3 (GDD5), 25.6 (MTCO) and 25.1 ka BP (AET/PET). The coincidence in timing of onset suggests that this corresponds to GS-3 [27,540 to 23,340 a b2k, 28], although the duration of the event at Monticchio is in this case shorter.

GDD5 showed a further rapid millennial increase during the millennium centred on 15.0 ka BP. This was paralleled by a marked increase in MTCO, centred on 15.3 ka BP, and preceded by the most rapid millennial increase in AET/PET that occurred during the millennium centred on 15.8 ka BP. In turn this was preceded by the most rapid millennial decrease in MTCO, centred on 16.5 ka BP, paralleled by a marked decrease in GDD5 centred on the same time. The changes in all three aspects of climate preceded by between a few centuries and a millennium the transition to GI-1 dated in Greenland ice cores to 14,692 a b2K [28]. Such patterns of leads and lags of different aspects of climate, and between

different locations and/or climatic sensors, can provide important insights into the climate dynamics that likely led to the climatic changes.

The most rapid millennial increase in MTCO was during the millennium centred on 12.5 ka BP. This lagged a moderate increase in GDD5 that peaked during the millennium centred on 13.1 ka BP but coincided with a small increase in AET/PET. Whereas the peak rate of increase in GDD5 corresponds to the onset of GI-1a at 13,099 a b2k [28], the peak rate of increase of MTCO falls during the GS-1 stadial that corresponds to the Younger Dryas cold stage. Once again this suggests that major climatic changes may have been time-transgressive between regions, with peak warming into the Holocene, and especially peak increase in winter temperatures, occurring several centuries earlier in Italy than in Greenland. The differences in timing of peak changes in MTCO and GDD5 also point to changes in seasonality as a key feature of the climatic changes taking place.

AET/PET shows the largest number of high signal to noise ratio peaks in rate of increase/decrease. Whilst some of these more or less coincide with, or shortly lead/lag, peaks in rate of increase/decrease of one or both of the temperature related variables (e.g. peak increase centred on 89.4 ka BP leading a peak increase in MTCO centred on 88.7 ka BP; peak increases centred on 27.7 and 15.8 ka BP already discussed above), others do not correspond to marked changes in either of the temperature variables. Notable amongst the latter are marked increases during the millennia centred on 55.2, 44.8 and 36.6 ka BP and marked decreases centred on 70.1, 58.5, 46.9, 42.7, 38.1 and 34.6 ka BP, increases generally corresponding to the onsets of interstadials and decreases to the onsets of stadials. Thus the most rapid millennial decrease in AET/PET was that during the millennium centred upon 70.1 ka BP. GDD5 and MTCO also decreased at about this time, with their most rapid millennial decreases centred on 70.2 and 69.8 ka BP respectively. These rapid decreases mark the end of a short-lived interstadial, the onset of which was marked by relatively rapid increases in all three climatic variables centred on 73.3 (MTCO), 73.0 (AET/PET) and 72.8 ka BP (GDD5). The duration and timing of the interstadial strongly suggest that it corresponds to GI-19.2 [72,340 to 70,380 a b2k, 28]. The longer duration, earlier onset and later end at Monticchio suggest that such events may reflect time-transgressive spatial shifts in key circulation features of the atmosphere and/or oceans.

Two further summaries of the climate histories are presented in Figure 5. The upper panels show the frequency, across the 2000 climate histories, with which the reconstructed climate falls in each cell of two-dimensional grids for each pair of bioclimatic variables. Whereas the MTCO vs GDD5 panel shows a single strong mode with a nearby secondary mode, the AET/PET vs GDD5 and AET/PET vs MTCO panels show strong elongation paralleling the AET/PET axis, and also clear evidence of two distinct climatic modes. The dominant mode is moister with lower GDD5 and higher MTCO, the secondary mode being drier with slightly higher GDD5 and more clearly lower MTCO.

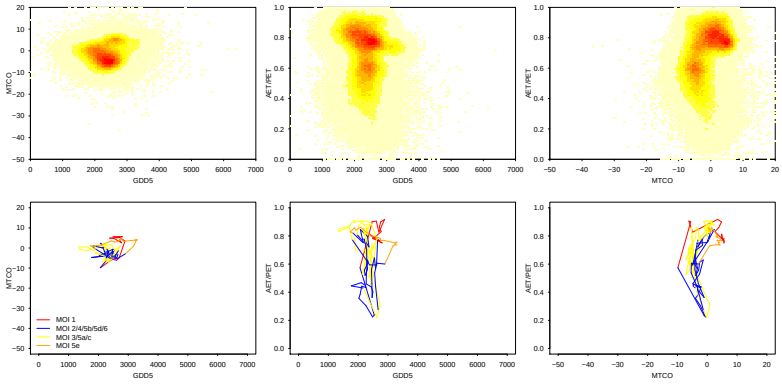

Figure 5: (Top row) A heatmap in bivariate climate showing the regions most visited by the climate histories. These are calculated by averaging across all climate histories to give a representative picture incorporating uncertainty. (Bottom row) A plot of the mean climate history in bivariate climate space, coloured according to Marine Oxygen Isotope stages.

The lower panels of Figure 5 show, for the same combinations of pairs of bioclimatic variables, the trajectory of the mean reconstructed climatic history. The lines showing the trajectories are coloured to indicate centuries that correspond approximately to the MOI stages and sub-stages. Four colours are used to distinguish the Holocene and late-glacial (MOI stage 1 and uppermost part of stage 2), the Last interglacial (MOI sub-stage 5e), the principal periods of glacial conditions (MOI stages 2 (remainder), 4 and 6 and sub-stages 5b and 5d) and the principal periods of interstadial conditions (MOI stage 3 and sub-stages 5a and 5c).

In terms of MTCO vs GDD5 the glacial and interstadial centuries are reconstructed to have generally lower MTCO values than the Holocene and last interglacial, with the exception of the late-glacial that is lumped with the Holocene but is markedly colder. Reconstructed GDD5 values for the Holocene are generally relatively high, whereas those for the last interglacial show three clusters at relatively low values, values similar to the Holocene and values higher than elsewhere in the record.

The Holocene and last interglacial also emerge as generally distinct in the AET/PET vs GDD5 plot. The last interglacial generally has lower reconstructed values for AET/PET than does the Holocene, the three clusters for GDD5 also showing a trend for the warmest centuries also to be the driest. The Holocene generally has high reconstructed AET/PET and moderate GDD5, with AET/PET markedly lower for the late-glacial period. The interstadial centuries have generally higher reconstructed AET/PET than the glacial cen-

turies, although because the simple categorisation used merges millennial timescale stadial and interstadial intervals within both the glacial intervals and MOI stage 3, there is considerable overlap. The principal mode seen in the panel above emerges as corresponding to interglacial and interstadial centuries, whilst the secondary mode predominantly corresponds to centuries classified as glacial. The long 'tail' extending to much lower AET/PET values also corresponds predominantly to glacial centuries.

The plot of AET/PET vs MTCO shows a further distinct pattern. Although the distinction between the Holocene and last interglacial is less clear than in the preceding panel, part of the Holocene is reconstructed to have the highest MTCO values for the entire period examined. The primary mode seen in the panel above again corresponds to the interglacial and a large proportion of the interstadial centuries, whilst the secondary mode again corresponds to glacial centuries. A striking feature of the plot, however, is how distinct from the remainder of the centuries are those of the latter part of the last glacial stage, these being characterised by reconstructed MTCO values lower than for most of the remainder of the record, and combinations of AET/PET and MTCO that lie outside the range spanned by other centuries of the record.

Key conclusions to emerge from these representations of the climate histories for Monticchio include: that there were distinct differences between Holocene and last interglacial climates; that Holocene climate was relatively stable, even when compared to that of the last interglacial; that the timing of the most rapid changes in the three bioclimatic variables differed; that there was no consistent pattern with respect to which climatic variable led or lagged when more than one showed a rapid change within the space of a few centuries; and that just two climatic modes have dominated during the past ca. 132 kyr, these being distinguished most strongly by differences in AET/PET.

6. Discussion

BClim presents a first attempt at a new approach to climate reconstruction from pollen at a single site. Much of the novelty arises from the use of climate histories. More deeply, the foundations of the underlying methods are rich forward models, which allow us to draw on realistic models of several processes, including climate, ecology and sedimentation. The mechanics draw on very modern algorithmic developments in statistical methods in Bayesian inference; as such the output histories have a direct and very rich probabilistic interpretation. This provides the basis for clear communication of uncertainty within the scientific community. All of these fields are separately under very active development. It can therefore be anticipated that future approaches to climate reconstruction from proxies will incorporate many of these features. The Bayesian architecture allows for the probabilistic combination, as a likelihood, of separate, probabilistically expressed, forward models. Nevertheless, it is at this stage limited to pollen cores from a single site. An expansion to multiple

cores, and thus to space-time histories is a natural next step. See [20] or [33] for a first step in this regard.

It is important to separate out the ideas presented in this paper (forward modelling, joint inference, climate histories) from the practicalities of the software Bclim. The former is broad, extendible, and applicable to a wide variety of reconstruction techniques. The latter at present is still simplistic in its nature. For example whilst the 28 pollen taxa used accounts for the majority of pollen in most surface and fossil pollen spectra used, larger quantities or different proxies could be combined into a forward model. Similarly the modern data and statistical models used by Bclim for calibrating pollen samples could better model the proportion dependence induced by the compositional nature of pollen counting. All these are avenues for future research.

6.1. Climate Histories

The immediate return from this first version of BClim is a file of histories. Such histories are jointly statistically consistent with all the available data, being here all the pollen and all the sources of chronological information. These permit rich user-defined summaries using whatever software is convenient. A very few of the possibilities have been illustrated. The ribbon plots will be the most familiar, being focussed on time-wise credible intervals. These intervals will be narrower than those generated by methods which use each slice separately to make statements about individual aspects of climate at times taken to correspond to the pollen data in that slice.

As attention turns to climate dynamics and to extremes, such histories will lend themselves to a multiplicity of novel alternative summaries. Examples here include: 'spaghetti plots' (e.g. Figure 5) which emphasise the past movement of the site within multidimensional climate space; plots that emphasise extrema in climate change; and plots focussing on bivariate climate. Files of histories for each of the two sites are available at the aforementioned package development website on GitHub. Readers are encouraged to explore these, recalling that all summaries have direct probabilistic interpretations. All histories are equally likely given all the data; but features which are common to many histories are more probable.

Even though the examples in Section 5 are intended as illustrative, they have led to some new insights. At Roya, the ribbon plots in Figure 1 have usefully resolved some anomalous results reported in earlier literature; but new questions have arisen on the date of the marked changes evident in some of the data. Figure 2 does not have a direct equivalent in other literature; it suggests that the marked changes in the three bioclimatic variables were time-transgressive. Figure 3 for Monticchio differs in detail from some previous reconstructions. But the new perspective offered by Figure 4 once again raises insights; here it is in the marked difference in variability that is apparent when comparing the

Holocene with the previous interglacial. But note that in all cases the probabilistic interpretation that can be placed on histories now provides much clearer uncertainty qualifications to accompany these insights.

The model of climate dynamics that has been used is very basic. It is simply a statistical characterisation of the 'stochastic smoothness' that is evident in, for example, the GISP records of δ^{18}O. This is 'minimally smooth', in the sense that climatic changes in small time intervals are mostly small, but can occasionally be very large indeed. Even this minimal smoothness is sufficient to generate the very considerable reduction in point-wise uncertainties that are exhibited by the ribbon plots, in comparison with those seen in the more primitive slice-by-slice reconstructions shown in blue. However, much richer deterministic models are available for palaeoclimate [see e.g. 11], though it would require further work to include these models in e.g. Bclim.

6.2. Forward Models

Bclim incorporates explicit forward models for two processes. The first of these underlies the first stage, slice-by-slice reconstructions. This is guided by ecological principles such as: at least three aspects of climate drive the ecological response seen in pollen; the relationship between climate and pollen productivity is not necessarily characterised by a simple model; pollen spectra typically exhibit very many zero counts. The incorporation of models of the dynamics of the ecological processes has not been modelled here, though this has been considered elsewhere [e.g. 17]. This is not trivial, and will be driven by further advances in statistical inference in situations where it is difficult to compute a likelihood.

The second forward model, BChron, is used by BClim to provide appropriate joint uncertainties for the chronologies and is built explicitly on a simple forward model of the sedimentation processes; namely that sedimentation rate is piece-wise constant, and subject to change at random times. This leads directly to a much more nuanced version of the linear interpolation that is widely used to date slices at depths other than those few that have been dated. Bchron inverts this forward model to create sedimentation histories. Other methods exist and, providing that they can be rendered within a Bayesian framework that can be used to generate stochastic sedimentation histories, can be incorporated into the Bclim framework.

6.3. Joint Statistical Inference

The final central message of this paper concerns joint inference, i.e. probabilistic statements about all aspects of a multivariate climate history, simultaneously, given all of the data. This is very naturally pursued within the Bayesian framework which is particularly well adapted for work on the inversion of systems that are built on forward models. For here the uncertainty in each model

cascades through the causal flow in a fashion that renders it simple to compute statistical likelihoods. The probabilistic inversion of these is the challenge that is being addressed by the recent advances in numerical algorithms and thus make Bayesian inference a natural paradigm in many fields.

The description given here of the Bclim algorithm emphasises the Monte Carlo trial and error procedure. However, the crude trial-and-error algorithm, as described figuratively in this paper, is inefficient. The technical version of this paper (P15) is in fact primarily focussed on numerical approximations that can reduce this inefficiency while retaining flexibility. These will initially be driven by developments in computing hardware; but the advances in numerical algorithms are to be anticipated. These may be particularity important in the future goal of space-time histories.

Acknowledgements

We would like to thank: the SUPRAnet group, led by Caitlin Buck; the members of the Isaac Newton Institute workshop on Uncertainty in Climate Prediction: Models, Methods and Decision Support; and the Past Earth Network for many informative discussions on these topics.

[1] Allen, J., W. Watts, E. McGee, and B. Huntley (2002). Holocene environmental variabilitythe record from Lago Grande di Monticchio, Italy. *Quaternary International 88*(1), 69–80.

[2] Allen, J. R. and B. Huntley (2009, jul). Last Interglacial palaeovegetation, palaeoenvironments and chronology: a new record from Lago Grande di Monticchio, southern Italy. *Quaternary Science Reviews 28*(15-16), 1521–1538.

[3] Allen, J. R., B. Huntley, and W. A. Watts (1996). The vegetation and climate of northwest Iberia over the last 14 000 yr. *Journal of Quaternary Science 11*, 125–147.

[4] Allen, J. R., W. A. Watts, and B. Huntley (2000, nov). Weichselian palynostratigraphy, palaeovegetation and palaeoenvironment; the record from Lago Grande di Monticchio, southern Italy. *Quaternary International 73-74*, 91–110.

[5] Allen, J. R. M., U. Brandt, A. Brauer, H.-W. Hubberten, B. Huntley, J. Keller, M. Kraml, A. Mackensen, J. Mingram, J. F. W. Negendank, N. R. Nowaczyk, H. Oberhänsli, W. A. Watts, S. Wulf, and B. Zolitschka (1999). Rapid environmental changes in southern Europe during the last glacial period. *Nature 400*, 740–743.

[6] Barndorff-Nielsen, O. E. (1997). Normal Inverse Gaussian distributions and stochastic volatility modelling. *Scandinavian Journal of Statistics 24*(1), 1–13.

[7] Bartlein, P. J., I. C. Prentice, and T. Webb (1986). Climatic surfaces from pollen data response for some eastern taxa North of. *Journal of Biogeography 13*(1), 35–57.

[8] Bernabo, J. C. (1981). Quantitative estimates of temperature changes over the last 2700 years in Michigan based on pollen data. *Quaternary Research 15*(2), 143–159.

[9] Blaauw, M. and J. A. Christen (2011). Flexible paleoclimate age-depth models using an autoregressive gamma process. *Bayesian Analysis 6*(3), 457–474.

[10] Bond, G. (1997). A Pervasive Millennial-Scale Cycle in North Atlantic Holocene and Glacial Climates. *Science 278*(5341), 1257–1266.

[11] Braconnot, P., S. P. Harrison, M. Kageyama, P. J. Bartlein, V. Masson-Delmotte, A. Abe-Ouchi, B. Otto-Bliesner, and Y. Zhao (2012, mar). Evaluation of climate models using palaeoclimatic data. *Nature Climate Change 2*(6), 417–424.

[12] Bradshaw, R. H. W. and O. Zackrisson (1990, aug). A two thousand year history of a northern Swedish boreal forest stand. *Journal of Vegetation Science 1*(4), 519–528.

[13] Brauer, A., J. R. M. Allen, J. Mingram, P. Dulski, S. Wulf, and B. Huntley (2007, jan). Evidence for last interglacial chronology and environmental change from Southern Europe. *Proceedings of the National Academy of Sciences of the United States of America 104*(2), 450–5.

[14] Bronk Ramsey, C. (2008). Deposition models for chronological records. *Quaternary Science Reviews 27*(1-2), 42–60.

[15] Cahill, N., A. C. Kemp, B. P. Horton, and A. C. Parnell (2015, oct). A Bayesian hierarchical model for reconstructing relative sea level: from raw data to rates of change. *Climate of the Past Discussions 11*(5), 4851–4893.

[16] Evans, M., S. Tolwinski-Ward, D. Thompson, and K. Anchukaitis (2013). Applications of proxy system modeling in high resolution paleoclimatology. *Quaternary Science Reviews 76*, 16–28.

[17] Garreta, V., P. A. Miller, J. Guiot, C. Hély, S. Brewer, M. T. Sykes, and T. Litt (2009). A method for climate and vegetation reconstruction through the inversion of a dynamic vegetation model. *Climate Dynamics 35*(2-3), 371–389.

[18] Haslett, J. and A. C. Parnell (2008). A simple monotone process with application to radiocarbon-dated depth chronologies. *Journal of the Royal Statistical Society, Series C 57*, 399–418.

[19] Haslett, J., M. Whiley, S. Bhattacharya, F. J. G. Mitchell, J. R. M. Allen, B. Huntley, S. P. Wilson, and M. Salter-Townshend (2006). Bayesian palaeoclimate reconstruction. *Journal of the Royal Statistical Society, Series A 169*, 395–438.

[20] Holmström, L., L. Ilvonen, H. Seppä, and S. Veski (2015, sep). A Bayesian spatiotemporal model for reconstructing climate from multiple pollen records. *The Annals of Applied Statistics 9*(3), 1194–1225.

[21] Huntley, B. (1993). The use of climate response surfaces to reconstruct palaeoclimate from Quaternary pollen and plant macrofossil data. *Philosophical Transactions of the Royal Society of London, Series B - Biological sciences. 341*, 215–223.

[22] Huntley, B., W. A. Watts, J. R. M. Allen, and B. Zolitschka (1999). Palaeoclimate, chronology and vegetation history of the Weichselian Lateglacial: comparative analysis of data from three cores at Lago Grande di Monticchio, southern Italy. *Quaternary Science Reviews 18*(7), 945–960.

[23] Lane, C. S., A. Brauer, S. P. E. Blockley, and P. Dulski (2013). Volcanic ash reveals time-transgressive abrupt climate change during the Younger Dryas. *Geology 41*(12), 1251–1254.

[24] Mann, M. E., Z. Zhang, M. K. Hughes, R. S. Bradley, S. K. Miller, S. Rutherford, and F. Ni (2008). Proxy-based reconstructions of hemispheric and global surface temperature variations over the past two millennia. *Proceedings of the National Academy of Sciences 105*, 13252–13257.

[25] Ohlwein, C. and E. R. Wahl (2012). Review of probabilistic pollen-climate transfer methods. *Quaternary Science Reviews 31*, 17–29.

[26] Parnell, A. C., J. Haslett, J. R. M. Allen, C. E. Buck, and B. Huntley (2008). A flexible approach to assessing synchroneity of past events using Bayesian reconstructions of sedimentation history. *Quaternary Science Reviews 27*(19-20), 1872–1885.

[27] Parnell, A. C., J. Sweeney, T. K. Doan, M. Salter-Townshend, J. R. M. Allen, B. Huntley, and J. Haslett (2015, jan). Bayesian inference for palaeoclimate with time uncertainty and stochastic volatility. *Journal of the Royal Statistical Society: Series C (Applied Statistics) 64*(1), 115–138.

[28] Rasmussen, S. O., M. Bigler, S. P. Blockley, T. Blunier, S. L. Buchardt, H. B. Clausen, I. Cvijanovic, D. Dahl-Jensen, S. J. Johnsen, H. Fischer, V. Gkinis, M. Guillevic, W. Z. Hoek, J. J. Lowe, J. B. Pedro, T. Popp, I. K. Seierstad, J. P. Steffensen, A. M. Svensson, P. Vallelonga, B. M. Vinther, M. J. Walker, J. J. Wheatley, and M. Winstrup (2014). A stratigraphic framework for abrupt climatic changes during the Last Glacial period based on three synchronized Greenland ice-core records: refining and extending the INTIMATE event stratigraphy. *Quaternary Science Reviews 106*, 14–28.

[29] Salter-Townshend, M. and J. Haslett (2012). Fast inversion of a flexible regression model for multivariate pollen counts data. *Environmetrics 23*(7), 595–605.

[30] Stuiver, M. (2000). GISP2 oxygen isotope ratios. *Quaternary Research 53*(3), 277–284.

[31] Sweeney, J. (2012). *Advances in Bayesian Model Development and Inversion in Multivariate Inverse Inference Problems with application to palaeoclimate reconstruction*. Ph. D. thesis, Trinity College Dublin.

[32] ter Braak, C. J. F. and S. Juggins (1993, oct). Weighted averaging partial least squares regression (WA-PLS): an improved method for reconstructing environmental variables from species assemblages. *Hydrobiologia 269-270*(1), 485–502.

[33] Tingley, M. P. and P. Huybers (2010). A Bayesian algorithm for reconstructing climate Anomalies in space and time. Part I: development and applications to paleoclimate reconstruction problems. *Journal of Climate 23*(10), 2759–2781.

[34] Tinner, W. and A. F. Lotter (2001). Central European vegetation response to abrupt climate change at 8.2 ka. *Geology 29*(6), 551.

[35] Tolwinski-Ward, S., M. Evans, M. Hughes, and K. Anchukaitis (2011). An efficient forward model of the climate controls on interannual variation in tree-ring width. *Climate Dynamics 36*(11), 2419–2439.

[36] Tolwinski-Ward, S. E., M. P. Tingley, M. N. Evans, M. K. Hughes, and D. W. Nychka (2014, apr). Probabilistic reconstructions of local temperature and soil moisture from tree-ring data with potentially time-varying climatic response. *Climate Dynamics 44*(3-4), 791–806.

[37] Vasko, K., H. T. T. Toivonen, and A. Korhola (2000). A Bayesian multinomial Gaussian response model for organism-based environmental reconstruction. *Journal of Palaeolimnology 24*, 243–250.

[38] Watts, W. A. (1985, jun). A long pollen record from Laghi di Monticchio, southern Italy: a preiminary account. *Journal of the Geological Society 142*(3), 491–499.

[39] Watts, W. A., J. R. M. Allen, and B. Huntley (1996). Vegetation history and palaeoclimate of the last glacial period at Lago Grande di Monticchio, southern Italy. *Quaternary Science Reviews 15*(2-3), 133–153.

[40] Williams, J. W., D. M. Post*, L. C. Cwynar, A. F. Lotter, and A. J. Levesque (2002). Rapid and widespread vegetation responses to past climate change in the North Atlantic region. *Geology 30*(11), 971.

[41] Wulf, S., M. Kraml, A. Brauer, J. Keller, and J. F. Negendank (2004, jan). Tephrochronology of the 100ka lacustrine sediment record of Lago Grande di Monticchio (southern Italy). *Quaternary International 122*(1), 7–30.

Appendix A. Chronology plots

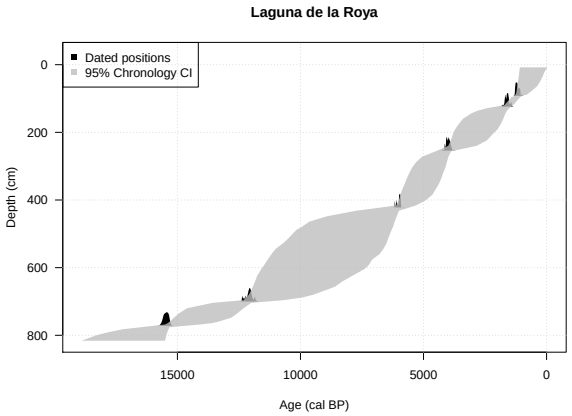

Figure A.6: Bchron chronology plot for Roya. There are 6 radiocarbon dates, with their calibrated histograms shown in black. The 95% credible interval for the chronology at each depth slice is shown in grey

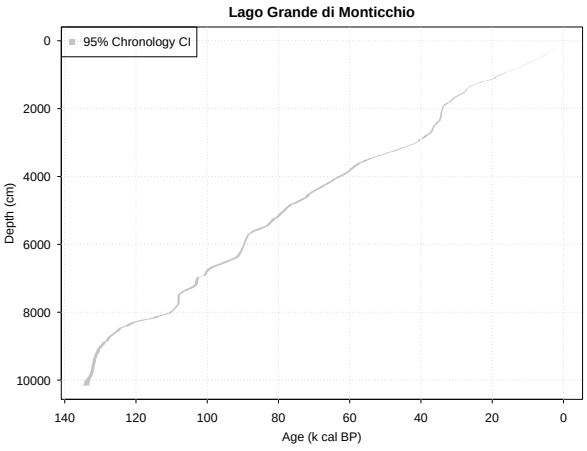

Figure A.7: Chronology plot for Monticchio. An error estimate of 1.5% was used to generate the chronology. The 95% credible interval for the chronology at each depth slice is shown in grey.

Appendix B. Pollen diagrams

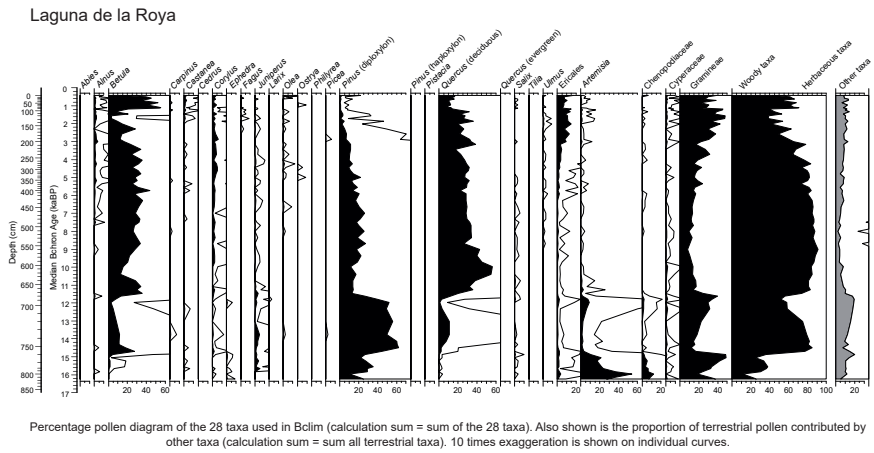

Percentage pollen diagram of the 28 taxa used in Bclim (calculation sum = sum of the 28 taxa). Also shown is the proportion of terrestrial pollen contributed by other taxa (calculation sum = sum all terrestrial taxa). 10 times exaggeration is shown on individual curves.

Figure B.8: Pollen diagram for Roya. The 28 taxa chosen for use in Bclim are those shown.

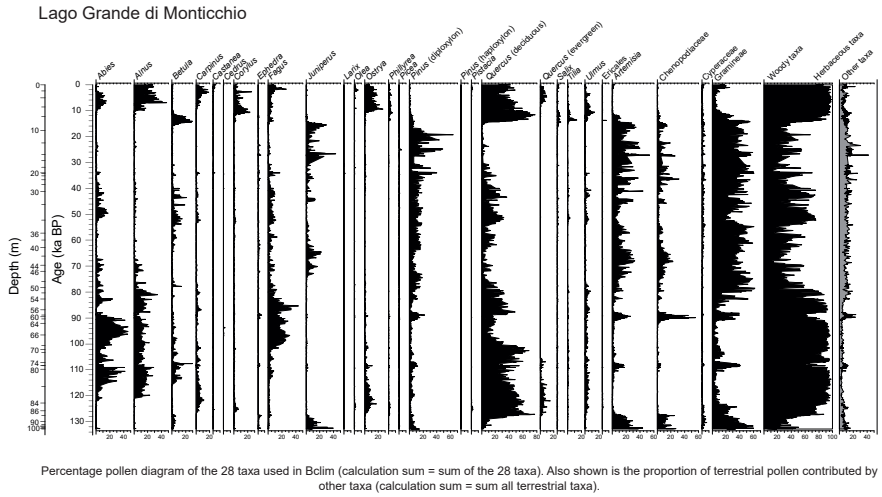

Percentage pollen diagram of the 28 taxa used in Bclim (calculation sum = sum of the 28 taxa). Also shown is the proportion of terrestrial pollen contributed by other taxa (calculation sum = sum all terrestrial taxa).

Figure B.9: Pollen diagram for Monticchio. The 28 taxa chosen for use in Bclim are those shown.